Yes-associated Protein Induces Age-dependent Inflammatory Signaling in the Pulmonary Endothelium

Memet T. Emin,[1] Alexandra M. Dubuisson,[1,2] Prisha Sujin Kumar,[1] Carsten Knutsen,[3] Cristina M. Alvira,[3] and Rebecca F. Hough*,[1]

[1]Pediatric Critical Care, Hospitalist, and Palliative Medicine, Department of Pediatrics, Columbia University Irving Medical Center, [2] Louisiana State University Health Sciences Center Shreveport, [3]Department of Pediatrics, University of California, San Francisco School of Medicine

*Address correspondence to:

Rebecca F. Hough

Department of Pediatrics

3959 Broadway, CHN10-24

New York, New York 10032, USA.

Phone: 212.305.2370

Email: rft2106@cumc.columbia.edu

ORCiD: 0000-0002-0203-4146

Conflict of interest statement: The authors have declared that no conflict of interest exists.

Running Title: Age-dependent YAP signaling in the lung endothelium

Data will be made available upon reasonable request.

Keywords: Acute Lung Injury, PARDS, lung endothelium, Yes-associated protein, NF-κB

Author contributions: MTE and RFH conceived this project. MTE, AMD, and RFH performed experiments. PSK, CK, and CMA analyzed data. RFH wrote and all authors edited and approved the manuscript.

Abstract

Acute Lung Injury (ALI) causes the highly lethal Acute Respiratory Distress Syndrome (ARDS) in children and adults, for which therapy is lacking. Children with Pediatric ARDS (PARDS) have a mortality rate that is about half of adults with ARDS. Improved ALI measures can be reproduced in rodent models with juvenile animals, suggesting that physiologic differences may underlie these outcomes. Here, we show that pneumonia-induced ALI caused inflammatory signaling in the endothelium of adult mice which depended on Yes-associated protein (YAP). This signaling was not present in 21-day-old weanling mice. Transcriptomic analysis of lung endothelial responses revealed nuclear factor kappa-B (NF-κB) as significantly increased with ALI in adult versus weanling mice. Blockade of YAP signaling protected against inflammatory response, hypoxemia, and NF-κB nuclear translocation in response to *Pseudomonas aeruginosa* pneumonia in adult mice. Our results demonstrate an important signaling cascade in the lung endothelium of adult mice that is not present in weanlings. We suggest other pathways may also exhibit age-dependent signaling, which would have important implications for ARDS therapeutics in the adult and pediatric age groups.

Introduction

Acute lung injury (ALI) causes the Acute Respiratory Distress Syndrome (ARDS) and Pediatric ARDS (PARDS). Mortality rates in adult patients with ARDS are double those of PARDS patients (1–3). Preclinical studies in rodents show decreased lung injury measures in juvenile mice (4–6), suggesting that age-specific physiological differences may underlie the distinct outcomes in ARDS and PARDS. Understanding the mechanisms of this differences may aid in the development of therapeutics for both age groups.

The Hippo pathway and its main effectors Yes-associated Protein (YAP) and PDZ-binding motif (TAZ) are vital for growth and differentiation (7–9). YAP is essential for the development of the endothelial barrier in the retina and brain (10), and interacts with tight junction components in the lung epithelium (11). Recently, YAP was shown to protect against lung injury (12, 13). Since YAP is developmentally important and implicated in ALI, we hypothesized that YAP responses to ALI could differ in juvenile and adult rodents.

Here, we show robust YAP protein expression in response to *Pseudomonas aeruginosa* infection in adult mice, but not in weanlings. YAP knockdown prevented the inflammatory response and hypoxemia in adult mice, suggesting a causal role of YAP in our injury model. Knockdown of YAP decreased nuclear translocation of NF-κB in adult mice, suggesting that YAP contributes to pro-inflammatory signaling in the pulmonary endothelium of adult but not juvenile mice.

Methods

Materials. For immunoblot, YAP mouse antibody (Cat#12395, 1:1000), YAP rabbit antibody (cat#14074, 1:1000), GAPDH mouse antibody (Cat#97166, 1:1000), and NF-κB p65 rabbit antibody (Cat#8242, 1:1000) were purchased from Cell Signaling Technology; HDAC1 mouse monoclonal antibody (Cat# 66085, 1:1000) was purchased from Proteintech; and actin rabbit antibody (cat# A2066, 1:1000) was purchased from Sigma-Aldrich. For lung cell isolation, CD31 rat monoclonal antibody clone MEC 13.3 (1:500, catalog 557355) was purchased from BD Biosciences. CD45 rat monoclonal antibody (1:600,

62 catalog 14-0451-85), CD41 rat monoclonal antibody (1:500, catalog 14-0411-85), and CD326 rat
63 monoclonal antibody (1:500, catalog 14-5791-85) were purchased from Invitrogen. siRNA construct
64 targeting Yap1 (siRNA ID #s76160) was purchased from ThermoFisher Scientific. Male and female
65 C57BL/6J mice were purchased from Jackson Laboratory (RRID:IMSR_JAX:000664). *P. aeruginosa*
66 strain K was obtained from Alice Prince (Columbia University). All protocols were reviewed and
67 approved by the Columbia University Institutional Animal Care and Use Committee.

68 *Pseudomonas-induced lung injury. P. aeruginosa* was prepared as previously described (14). We
69 anesthetized mice and intranasally (i.n.) instilled 2.5 x 10^5 colony forming units (CFUs) *P. aeruginosa* at
70 exponential growth phase in 50µl sterile PBS (adult) or 20µl (weanling). 24 hours later, we anesthetized
71 the mice, performed a tracheotomy, and collected BAL as described (14). We retained lungs after BAL for
72 downstream experiments. Extra-vascular lung water (EVLW) was measured as described (14, 15).

73 *SpO_2 measurement*. For non-invasive O_2 saturation (SpO_2) measurements, we anesthetized mice and
74 removed the fur from right thigh. We placed a MouseOx® Pulse Oximeter sensor (Starr Life Sciences
75 Corp, Oakmont, PA) on the right femoral artery region and recorded SpO_2 after a 15-min stabilization
76 period.

77 *YAP RT-PCR.* We isolated RNA from whole lung using miRNeasy kit (Qiagen) according to the
78 manufacturer's protocol. 250ng of RNA was reverse-transcribed into cDNA. We performed quantitative
79 PCR using TaqMan Gene Expression Master Mix with QuantStudio™ 5 Real-Time PCR Instrument
80 (Thermo Fisher Scientific Applied Biosystems). The following primers were used: Yap1: Assay ID
81 Mm01143263_m1 and Actb: Assay ID Mm02619580_g1 (ThermoFisher).

82 *YAP knockdown.* Anesthetized mice were in vivo transfected with YAP siRNA (50µg in 150µL) by tail
83 vein injection 24 hours before *P. aeruginosa* instillation.

84 *Immunoblot.* Without freezing samples, we enriched lungs for cytoplasmic and nuclear fractions using
85 NE-PER Nuclear and Cytoplasmic Extraction Reagents (Thermo Fisher Scientific, cat #78833). Equal
86 amounts of protein were separated by SDS-PAGE, transferred onto nitrocellulose membrane, blocked in

87 StartingBlock Blocking Buffer (Thermo Scientific / Pierce, catalog 37543), and immunoblotting was
88 performed.

89 *Endothelial cell isolation.* Endothelial cells from C57BL/6J mice were isolated as described (16, 17) with
90 the following modifications. Lungs were digested for 15 min at 37°C in 0.38mg/ml Liberase (Roche) in
91 D-PBS + 0.1% albumin. We used a DynaMag-2 Magnet and Dynabeads Sheep Anti-Rat IgG (Invitrogen)
92 to deplete CD45+ and CD41+ cells, then positively enrich three times for CD31+ cells. These procedures
93 yielded ~10^5 CD31+ cells per mouse lung with <5% leukocyte contamination.

94 *Bulk RNA-sequencing.* RNA was isolated from freshly isolated endothelial cells bound to magnetic beads
95 (miRNeasy). RNA-sequencing was performed by Azenta. We aligned sequences to the GRCm39 mouse
96 genome using STAR aligner (v2.10.a) (18). We analyzed differential gene expression (DE) with EdgeR
97 (3.38.4) (19) using a generalized linear model with thresholds for significance set at <0.05 FDR
98 (Benjamani-Hochenberg) and 1>|Log2(FC)|. Pathway analysis was performed using Metascape (v3.5)
99 (20), using up- and down-regulated genes separately. Code for this analysis can be found at
100 https://github.com/CarstenKnutsen/bulkrnaseq_pseudomonas_lung_ec/.

101 **Results**

102 *Differential lung injury responses in weanling and adult mice.*

103 To determine lung injury responses, we intranasally instilled weanling (P21-24) and adult (8-10 week old)
104 mice with *P. aeruginosa*. Twenty-four hours later, we assessed mice for lung injury by measurement of
105 BAL protein, BAL cell count, BAL neutrophils, EVLW, BAL cytokines, and non-invasive measurement
106 of SpO_2. Following *P. aeruginosa* instillation, adult mice had an increase in BAL protein, BAL cell count,
107 BAL neutrophils, EVLW, BAL Il-6 and BAL TNF-α (**Fig 1A-E**), and a decrease in SpO_2 (**Fig 1F**)
108 compared to weanling mice. Saline treatment did not produce different responses in any lung injury
109 measurements.

110 Given the difference in size of the weanling and adult mice (~10g vs. ~25g), we considered whether
111 delivery of *P. aeruginosa* could differ between the two age groups. We also assessed for altered clearance

112 of *P. aeruginosa*, as decreased clearance of *P. aeruginosa* has been noted in mice <20 days old (21). To
113 assess *P. aeruginosa* delivery, we instilled the same number of CFUs in the same volume to both age
114 groups, and again in two different volumes. The lung injury results did not differ when the volume was
115 changed. To assess bacterial clearance, we measured BAL CFUs 24h after instillation and noted no
116 difference between the two age groups (**Supplemental Fig 1-**
117 **https://figshare.com/s/5e58428fdf883f37fe84**). These findings suggest that a similar number of CFUs
118 was delivered in both ages and that bacterial clearance did not differ between the age groups.

119 *P. aeruginosa-induced changes in YAP protein expression differ with age*

120 We determined changes in expression of YAP in response to *P. aeruginosa*-induced lung injury. Following
121 BAL and a vascular wash, we enriched whole lungs from *P. aeruginosa*- and saline-treated mice into
122 nuclear and cytoplasmic portions. We found that adult mice had robust increases in YAP protein
123 expression in response to *P. aeruginosa* instillation in both cytoplasmic and nuclear fractions (**Fig 2A, B**).
124 In contrast, weanling mice had decreased cytoplasmic expression of YAP and no change in nuclear
125 expression. Of note, there was no difference in YAP protein expression between age groups in saline-
126 treated controls (**Supplemental Fig 2**), suggesting that baseline YAP expression does not differ between
127 the two age groups. We assessed YAP mRNA expression with RT-PCR and noted that YAP mRNA
128 expression in both weanling and adult mice decreased upon *P. aeruginosa*-induced injury (**Supplemental**
129 **Fig 3**), suggesting a post-transcriptional mechanism of increased YAP protein expression in adult mice.

130 *P. aeruginosa-induced YAP protein increases occur in lung endothelial cells*

131 Given the substantial increase in inflammatory cells in the BAL of adult versus weanling mice (**Fig 1B-**
132 **C**), we considered whether leukocyte expression of YAP (22) contributed to YAP increases in adult mice.
133 To determine the cell type in which YAP expression increased, we enriched lungs for three fractions:
134 endothelial cells, epithelial cells, and leukocytes plus platelets. We performed immunoblot for YAP in
135 each of the enriched cell populations. We noted an increase in YAP protein expression in endothelial cells
136 (**Fig 2C**). There was no significant increase in YAP expression in epithelial cells (**Fig 2D**), and no YAP

137 protein expression was detected in the leukocyte- and platelet-enriched fraction in PBS or *P. aeruginosa*-
138 treated mice. These data suggest that YAP increases in lung endothelial cells are the main driver of the
139 increased YAP in adult mice.

140 *Vascular YAP mediates P. aeruginosa-induced lung injury in adult mice*

141 Since YAP expression increases in adult mice, but not in weanling mice, we hypothesized that adult mice
142 exhibit YAP-dependent lung injury responses that weanling mice lack. Thus, we targeted endothelial YAP
143 in adult mice by tail vein injection of siRNA-targeted YAP. Injection of YAP-targeted siRNA decreased
144 YAP expression in *P. aeruginosa* infected mice by ~80% (**Fig 3A**). We assessed lung injury measures as
145 in **Fig 1** and found that YAP knockdown prevented *P. aeruginosa*-induced increases in BAL cell count
146 and IL-6, as well as *P. aeruginosa*-induced decreases in SpO_2 (**Fig 3B-D**). This suggests that endothelial
147 YAP expression is important for inflammatory and physiological responses in *P. aeruginosa*-induced lung
148 injury. Notably, YAP knockdown had no effect on BAL protein and EVLW, suggesting that endothelial
149 YAP may not be essential for barrier failure.

150 *YAP expression drives endothelial NF-κB responses in P. aeruginosa-infected adult mice*

151 To determine differences in *P. aeruginosa*-induced lung injury endothelial responses between weanling
152 and adult mice, we performed bulk RNA sequencing on freshly isolated endothelial cells from mice
153 treated with i.n. *P. aeruginosa* and control mice treated with PBS. Gene expression differences between
154 both age groups did not differ greatly under control conditions (107 genes upregulated; 128
155 downregulated, **Fig 4A, Supplemental data files, Gene Expression Omnibus GSE291989**). However,
156 gene expression responses to *Pseudomonas*-induced lung injury differed greatly between the age groups
157 (966 upregulated; 1474 downregulated). This suggests substantial differences in lung endothelial
158 responses to inflammatory injury of weanling and adult mice.

159 Of note, there was no significant alteration in *Yap1* gene expression with *P. aeruginosa* instillation in
160 either weanling or adult endothelia, consistent with our RT-PCR results (**Supplemental Fig 3**). We

161 identified pathways that exhibited increased expression in adult mice in response to *P. aeruginosa*-
162 induced lung injury relative to weanling mice. The most significant increases were found in TNFα
163 signaling via NF-κB (specific genes: *Klf9*, *Cdkn1a*, *Map3k8*, *Rcan1*, *Ets2*, *Hes1*, *Gadd45b*, *Nfkbia*,
164 *Nr4a2*, *Per1*, *Plaur*, *Tgif1*, *Socs3*, *Ccrl2*, *Plk2*, *Kdm6b*, *Ppp1r15a*, *Maff*, *Ccnl1*, *Zbtb10*, *Sik1*, **Fig 4B,**
165 **Supplemental data files**). Although both weanling and adult endothelial cells increased their expression
166 of genes involved in this pathway, the adult endothelial responses were increased relative to responses in
167 weanling mice.

168 We considered whether YAP drove NF-κB nuclear translocation in endothelia, leading to a more robust
169 inflammatory response in adult mice. First, we determined whether *P. aeruginosa* instillation drove NF-
170 κB translocation to the nucleus in adult mice. 24h after *P. aeruginosa* instillation, we enriched whole lung
171 into nuclear and cytoplasmic fractions. We noted a significant increase in NF-κB in the nuclear fraction
172 and a decrease in the cytoplasmic fraction (**Fig 4C**). In weanlings, there was an increase in NF-κB in the
173 nuclear fraction, but no significant difference in NF-κB quantity in the cytoplasmic fraction upon
174 instillation of *P. aeruginosa* (**Supplemental Fig 4**), suggesting that NF-κB nuclear translocation in
175 response to *P. aeruginosa* in weanlings may be decreased in comparison to adult mice. To determine
176 whether the increase in YAP expression in adult mice drove NF-κB translocation, we knocked down YAP
177 expression by vascular injection of siRNA as in **Fig 3A** and instilled *P. aeruginosa* into control- and
178 siRNA-treated mice 24h later. 24 hours after *P. aeruginosa* instillation, we measured NF-κB in the
179 nuclear and cytoplasmic fractions. We noted that YAP knockdown increased NF-κB protein expression in
180 the cytoplasm and decreased NF-κB expression in the nucleus (**Fig 4D**), suggesting that YAP mediated
181 NF-κB nuclear translocation.

182 **Discussion**

183 Although pneumonia is a common cause of ARDS and PARDS, ALI signaling including barrier failure
184 and infiltration of inflammatory cells that ultimately leads to hypoxemia is orchestrated by the

185 microvascular endothelium (15, 23). Here, we present a novel mechanism of age-dependent signaling in
186 the pulmonary endothelium. Our data suggest that in adult mice YAP-dependent inflammatory signaling
187 contributes to ALI, worsening outcomes. One possibility is that bacterial clearance of *P. aeruginosa*
188 differs in the two age groups. Indeed, decreased clearance of *P. aeruginosa* has been noted in mice >20
189 days old (21). While we did see decreased neutrophilic infiltration in weanling mice (**Fig 1C**), there was
190 no significant difference in BAL colony forming units at 24h (**Supplemental Fig 1**), suggesting that
191 bacterial clearance did not differ significantly between the age groups.
192 Previously work using models of indirect lung injury showed that endothelial YAP protected against lung
193 injury. Indeed, YAP inhibited NF-κB nuclear translocation by promoting degradation of tumor necrosis
194 factor receptor-associated factor 6 (TRAF-6) in these models (13). In the epithelium, nuclear YAP may
195 increase *ikba* gene expression, also inhibiting NF-κB nuclear translocation (24). Endothelial YAP was
196 also recently shown to protect against lung injury secondary high-tidal volume ventilation (12). In our
197 transcriptomics dataset, expression of the *ikba* mouse homologue *nfkbia* was induced in both weanling
198 and adult mice, supporting YAP-independent drivers of transcription. It is well-known that YAP has a
199 pleiotropic role in lung injury and repair. We suggest that knockdown, rather than knockout of YAP used
200 in these prior studies, more accurately reflects a possible pharmacological inhibition of YAP that could be
201 used in pre-clinical and/or clinical trials. Furthermore, complete inhibition of YAP raises concerns about
202 the effects on development, differentiation, and repair that are attributed to YAP. Indeed, it is possible that
203 YAP knockout leads to up-regulation of alternative pathways (25). Our work suggests that the role of YAP
204 in lung injury and repair is complex and requires further study.
205 In neonatal mice in the early alveolar stage of lung development, NF-κB is known to play a protective
206 role, ultimately promoting angiogenesis (17, 26–28). To our knowledge, this role has not been described
207 in weanling mice in the late alveolar stage used in our study. However, it is possible that NF-κB nuclear
208 translocation in weanling mice results in signaling that differs from canonical pro-inflammatory signaling
209 in adults.

Our study has limitations. First, the signaling that leads to differential YAP expression between the weanling and adult age groups is unclear. Our RT-PCR (**Supplemental Fig 3**) and transcriptomics data suggest that the regulation is post-transcriptional, yet the drivers of these differences remain unknown. Second, our bulk RNA sequencing data do not reveal the specific endothelial cell types that drive the inflammatory responses. We and others have identified the post-capillary venule as a primary location of inflammatory signaling (29–33, 14). However, a gene expression signature of this cell type to our knowledge remains elusive. Finally, the mechanism(s) by which YAP drives NF-κB nuclear translocation in adult mice remains unclear. This deserves further investigation.

Here, we show evidence for novel age-dependent inflammatory signaling in the pulmonary endothelium. Our work suggests that targeting of YAP-dependent endothelial signaling may be helpful in the prevention and treatment of ARDS but may be detrimental in PARDS. Our transcriptomics dataset suggests numerous differences in inflammatory responses in the pulmonary endothelium between weanling and adult age groups, of which YAP-driven NF-κB is but one example. Further investigation into age-dependent mechanisms of lung injury could aid in the tailoring of therapies across the lifespan.

Grants

This work was supported by NIH K08HL148403; a Stony Wold-Herbert Fund Grant-in-aid; and a Columbia University Department of Pediatrics Innovation Nucleation Fund Award (R.F.H.).

Acknowledgements

We are grateful to Jahar Bhattacharya, Wellington V. Cardoso, Mohammad N. Islam, and Galina Gusarova for contributive discussions.

231 **Figure Legends**

232 **Figure 1. Responses to intranasal *Pseudomonas aeruginosa* in weanling and adult mice.** Analyses
233 were performed 24h after intranasal instillation of 2.5 x 10^5 CFU of *P. aeruginosa* or PBS. (**A-C, E**) BAL
234 was obtained by instillation of ice cold PBS intratracheally. (**A**) BAL protein was determined by BCA
235 assay. (**B-C**) BAL cell and neutrophil counts were determined with Vetscan hematology analyzer. (**D**)
236 ELVW was determined in separate experiments. (**E**) BAL cytokines were measured by multiplex array
237 (Eve Technologies). (**F**) SpO_2 was determined in anesthetized mice using a MouseOx® Pulse Oximeter.
238 Data are shown as mean±SE. Number of replicates are indicated by dots (≥4 for all groups). *BAL*,
239 bronchoalveolar lavage; *3wo*, 3 week-old mice; *Pseudomonas*, *Pseudomonas aeruginosa* strain K*; PMNs*,
240 neutrophils; *EVLW*, extravascular lung water; *IL-6*, interleukin-6; *TNF-α*, tumor necrosis factor α; SpO_2,
241 non-invasive O_2 saturation. *p<0.05, **p<0.01, ***p<0.001, ****p<0.0001. Multiple comparisons were
242 analyzed by two-way ANOVA; paired differences were compared by unpaired 2-tailed t test.
243

244 **Figure 2. YAP expression responses to *P. aeruginosa*-induced lung injury in weanling and adult**
245 **mice.** Representative gels and scatter plots show immunoblotting and densitometry of enriched
246 cytoplasmic (**A**) and nuclear (**B**) fractions of whole lung, and enriched lung endothelial cells (**C**) and
247 epithelial cells (**D**). All animals were treated with i.n. PBS or *P. aeruginosa* 24 hours before lung removal.
248 Antibodies used were YAP rabbit monoclonal, GAPDH mouse monoclonal, HDAC mouse monoclonal,
249 and actin rabbit polyclonal. Lanes were run on the same gel. Number of replicates are indicated by dots
250 (≥4 for all groups). *3wo*, 3 week-old mice; *n.s.*, not significant. *$p < 0.05$, ****$p<0.0001$. Differences
251 between groups were compared by t test.

252

253 **Figure 3. YAP mediates *P. aeruginosa*-induced lung injury in adult mice.** Mice were injected
254 intravenously with YAP-targeted siRNA or non-targeting control siRNA (NTC) 24h before all mice were
255 treated with *P. aeruginosa* intranasal instillation. (**A**) Representative gel and scatter plots show
256 immunoblotting and densitometry of whole lung cytoplasmic fraction. Antibodies used were YAP rabbit
257 monoclonal and GAPDH mouse monoclonal. There was high variability of lung YAP expression, but
258 statistical significance remained when the highest outlier from the NTC-treated group was removed from
259 the analysis. (**B**) BAL cell counts were determined with Vetscan hematology analyzer. (**C**) BAL IL-6 was
260 measured by multiplex array. (**D**) SpO_2 was determined using a MouseOx® Pulse Oximeter. Number of
261 replicates are indicated by triangles (≥3 for all groups). *BAL*, bronchoalveolar lavage; *3wo*, 3 week-old
262 mice; *IL-6*, interleukin-6; *TNF-α*, tumor necrosis factor α; SpO_2, non-invasive O_2 saturation. *$p<0.05$,
263 ***$p<0.001$, ****$p<0.0001$. Paired differences were compared by t test.
264

265 **Figure 4. YAP expression drives endothelial NF-κB responses in *P. aeruginosa*-infected adult mice.**
266 (**A**) Principal component analysis of four treatment groups. *PC1*, principal component 1; *blue*, saline-
267 treated; *orange*, *P. aeruginosa*-treated. •, adult; **x**, weanling. (**B**) Top pathways in which adult response to
268 *P. aeruginosa* instillation is higher than in weanling mice. (**C**) Representative gel and scatter plots show
269 immunoblotting and densitometry of whole lung cytoplasmic and nuclear enriched fractions: (**C**) 24h
270 after PBS or *P. aeruginosa* instillation and (**D**) following pretreatment with YAP siRNA by tail vein
271 injection and *P. aeruginosa* instillation. Antibodies used were NF-κB p65 rabbit monoclonal, YAP rabbit
272 monoclonal, HDAC mouse monoclonal, and actin rabbit polyclonal. Number of replicates are indicated
273 by dots (≥3 for all groups). *NF-κB,* nuclear factor-kappa B*; NTC,* non-targeting control siRNA*; siRNA,*
274 YAP-targeted siRNA. *$p<0.05$, **$p<0.01$, ***$p<0.001$, ****$p<0.0001$. Paired differences were compared
275 by t test.
276

References

1. **Dowell JC**, **Parvathaneni K**, **Thomas NJ**, **Khemani RG**, **Yehya N**. Epidemiology of Cause of Death in Pediatric Acute Respiratory Distress Syndrome. *Crit Care Med* 46: 1811–1819, 2018. doi: 10.1097/CCM.0000000000003371.

2. **Matthay MA**, **Zemans RL**, **Zimmerman GA**, **Arabi YM**, **Beitler JR**, **Mercat A**, **Herridge M**, **Randolph AG**, **Calfee CS**. Acute respiratory distress syndrome. *Nat Rev Primer* 5: 18, 2019. doi: 10.1038/s41572-019-0069-0.

3. **Schouten LR**, **van Kaam AH**, **Kohse F**, **Veltkamp F**, **Bos LD**, **de Beer FM**, **van Hooijdonk RT**, **Horn J**, **Straat M**, **Witteveen E**, **Glas GJ**, **Wieske L**, **van Vught LA**, **Wiewel MA**, **Ingelse SA**, **Cortjens B**, **van Woensel JB**, **Bos AP**, **Walther T**, **Schultz MJ**, **Wösten-van Asperen RM**. Age-dependent differences in pulmonary host responses in ARDS: a prospective observational cohort study. *Ann Intensive Care* 9: 55, 2019. doi: 10.1186/s13613-019-0529-4.

4. **Smith LS**, **Gharib SA**, **Frevert CW**, **Martin TR**. Effects of age on the synergistic interactions between lipopolysaccharide and mechanical ventilation in mice. *Am J Respir Cell Mol Biol* 43: 475–486, 2010. doi: 10.1165/rcmb.2009-0039OC.

5. **Schouten LRA**, **Helmerhorst HJF**, **Wagenaar GTM**, **Haltenhof T**, **Lutter R**, **Roelofs JJTH**, **van Woensel JBM**, **van Kaam AHLC**, **Bos AP**, **Schultz MJ**, **Walther T**, **Wösten-van Asperen RM**. Age-Dependent Changes in the Pulmonary Renin-Angiotensin System Are Associated With Severity of Lung Injury in a Model of Acute Lung Injury in Rats. *Crit Care Med* 44: e1226–e1235, 2016. doi: 10.1097/CCM.0000000000002008.

6. **Ingelse SA**, **Juschten J**, **Maas MAW**, **Matute-Bello G**, **Juffermans NP**, **van Woensel JBM**, **Bem RA**. Fluid restriction reduces pulmonary edema in a model of acute lung injury in mechanically ventilated rats. *PLoS One* 14: e0210172, 2019. doi: 10.1371/journal.pone.0210172.

7. **Totaro A**, **Panciera T**, **Piccolo S**. YAP/TAZ upstream signals and downstream responses. *Nat Cell Biol* 20: 888–899, 2018. doi: 10.1038/s41556-018-0142-z.

8. **Zou R**, **Xu Y**, **Feng Y**, **Shen M**, **Yuan F**, **Yuan Y**. YAP nuclear-cytoplasmic translocation is regulated by mechanical signaling, protein modification, and metabolism. *Cell Biol Int* 44: 1416–1425, 2020. doi: 10.1002/cbin.11345.

9. **van Soldt BJ**, **Cardoso WV**. Hippo-Yap/Taz signaling: Complex network interactions and impact in epithelial cell behavior. *Wiley Interdiscip Rev Dev Biol* 9: e371, 2020. doi: 10.1002/wdev.371.

10. **Kim J**, **Kim YH**, **Kim J**, **Park DY**, **Bae H**, **Lee DH**, **Kim KH**, **Hong SP**, **Jang SP**, **Kubota Y**, **Kwon YG**, **Lim DS**, **Koh GY**. YAP/TAZ regulates sprouting angiogenesis and vascular barrier maturation. *J Clin Invest* 127: 3441–3461, 2017. doi: 10.1172/JCI93825.

11. **Zhou B**, **Flodby P**, **Luo J**, **Castillo DR**, **Liu Y**, **Yu F-X**, **McConnell A**, **Varghese B**, **Li G**, **Chimge N-O**, **Sunohara M**, **Koss MN**, **Elatre W**, **Conti P**, **Liebler JM**, **Yang C**, **Marconett CN**, **Laird-Offringa IA**, **Minoo P**, **Guan K**, **Stripp BR**, **Crandall ED**, **Borok Z**. Claudin-18-mediated YAP activity regulates lung stem and progenitor cell homeostasis and tumorigenesis. *J Clin Invest* 128: 970–984, 2018. doi: 10.1172/JCI90429.

12. **Su K**, **Wang J**, **Lv Y**, **Tian M**, **Zhao Y-Y**, **Minshall RD**, **Hu G**. YAP Expression in Endothelial Cells Prevents Ventilator-induced Lung Injury. .

13. **Lv Y**, **Kim K**, **Sheng Y**, **Cho J**, **Qian Z**, **Zhao Y-Y**, **Hu G**, **Pan D**, **Malik AB**, **Hu G**. YAP Controls Endothelial Activation and Vascular Inflammation Through TRAF6. *Circ Res* 123: 43–56, 2018. doi: 10.1161/CIRCRESAHA.118.313143.

14. **Emin MT**, **Lee MJ**, **Bhattacharya J**, **Hough RF**. Mitochondria of lung venular capillaries mediate lung-liver cross talk in pneumonia. *Am J Physiol Lung Cell Mol Physiol* 325: L277–L287, 2023. doi: 10.1152/ajplung.00209.2022.

15. **Hough RF**, **Islam MN**, **Gusarova GA**, **Jin G**, **Das S**, **Bhattacharya J**. Endothelial mitochondria determine rapid barrier failure in chemical lung injury. *JCI Insight* 4, 2019. doi: 10.1172/jci.insight.124329.

16. **Schmidt EP**, **Yang Y**, **Janssen WJ**, **Gandjeva A**, **Perez MJ**, **Barthel L**, **Zemans RL**, **Bowman JC**, **Koyanagi DE**, **Yunt ZX**, **Smith LP**, **Cheng SS**, **Overdier KH**, **Thompson KR**, **Geraci MW**, **Douglas IS**, **Pearse DB**, **Tuder RM**. The pulmonary endothelial glycocalyx regulates neutrophil adhesion and lung injury during experimental sepsis. *Nat Med* 18: 1217–23, 2012. doi: 10.1038/nm.2843.

17. **Liu M**, **Iosef C**, **Rao S**, **Domingo-Gonzalez R**, **Fu S**, **Snider P**, **Conway SJ**, **Umbach GS**, **Heilshorn SC**, **Dewi RE**, **Dahl MJ**, **Null DM**, **Albertine KH**, **Alvira CM**. Transforming Growth Factor-induced Protein Promotes NF-κB-mediated Angiogenesis during Postnatal Lung Development. *Am J Respir Cell Mol Biol* 64: 318–330, 2021. doi: 10.1165/rcmb.2020-0153OC.

18. **Dobin A**, **Davis CA**, **Schlesinger F**, **Drenkow J**, **Zaleski C**, **Jha S**, **Batut P**, **Chaisson M**, **Gingeras TR**. STAR: ultrafast universal RNA-seq aligner. *Bioinformatics* 29: 15–21, 2013. doi: 10.1093/bioinformatics/bts635.

19. **Robinson MD**, **McCarthy DJ**, **Smyth GK**. edgeR: a Bioconductor package for differential expression analysis of digital gene expression data. *Bioinformatics* 26: 139–140, 2010. doi: 10.1093/bioinformatics/btp616.

20. **Zhou Y**, **Zhou B**, **Pache L**, **Chang M**, **Khodabakhshi AH**, **Tanaseichuk O**, **Benner C**, **Chanda SK**. Metascape provides a biologist-oriented resource for the analysis of systems-level datasets. *Nat Commun* 10: 1523, 2019. doi: 10.1038/s41467-019-09234-6.

21. **Sordelli DO**, **Djafari M**, **García VE**, **Fontán PA**, **Döring G**. Age-dependent pulmonary clearance of Pseudomonas aeruginosa in a mouse model: diminished migration of polymorphonuclear leukocytes to N-formyl-methionyl-leucyl-phenylalanine. *Infect Immun* 60: 1724–1727, 1992. doi: 10.1128/iai.60.4.1724-1727.1992.

22. **Meli VS**, **Atcha H**, **Veerasubramanian PK**, **Nagalla RR**, **Luu TU**, **Chen EY**, **Guerrero-Juarez CF**, **Yamaga K**, **Pandori W**, **Hsieh JY**, **Downing TL**, **Fruman DA**, **Lodoen MB**, **Plikus MV**, **Wang W**, **Liu WF**. YAP-mediated mechanotransduction tunes the macrophage inflammatory response. *Sci Adv* 6: eabb8471, 2020. doi: 10.1126/sciadv.abb8471.

23. **Hough RF**, **Bhattacharya S**, **Bhattacharya J**. Crosstalk signaling between alveoli and capillaries. *Pulm Circ* 8: 2045894018783735, 2018. doi: 10.1177/2045894018783735.

24. **LaCanna R**, **Liccardo D**, **Zhang P**, **Tragesser L**, **Wang Y**, **Cao T**, **Chapman HA**, **Morrisey EE**, **Shen H**, **Koch WJ**, **Kosmider B**, **Wolfson MR**, **Tian Y**. Yap/Taz regulate alveolar regeneration and resolution of lung inflammation. *J Clin Invest* 129: 2107–2122, 2019. doi: 10.1172/JCI125014.

25. **Moroishi T**, **Park HW**, **Qin B**, **Chen Q**, **Meng Z**, **Plouffe SW**, **Taniguchi K**, **Yu F-X**, **Karin M**, **Pan D**, **Guan K-L**. A YAP/TAZ-induced feedback mechanism regulates Hippo pathway homeostasis. *Genes Dev* 29: 1271–1284, 2015. doi: 10.1101/gad.262816.115.

26. **Alvira CM**, **Abate A**, **Yang G**, **Dennery PA**, **Rabinovitch M**. Nuclear Factor-κB Activation in Neonatal Mouse Lung Protects against Lipopolysaccharide-induced Inflammation. *Am J Respir Crit Care Med* 175: 805–815, 2007. doi: 10.1164/rccm.200608-1162OC.

27. **Iosef C**, **Alastalo T-P**, **Hou Y**, **Chen C**, **Adams ES**, **Lyu S-C**, **Cornfield DN**, **Alvira CM**. Inhibiting NF-κB in the developing lung disrupts angiogenesis and alveolarization. *Am J Physiol - Lung Cell Mol Physiol* 302: L1023–L1036, 2012. doi: 10.1152/ajplung.00230.2011.

28. **Alvira CM**. Nuclear factor-kappa-B signaling in lung development and disease: one pathway, numerous functions. *Birt Defects Res A Clin Mol Teratol* 100: 202–216, 2014. doi: 10.1002/bdra.23233.

29. **Schneeberger EE**. Segmental differentiation of endothelial intercellular junctions in intra-acinar arteries and veins of the rat lung. *Circ Res* 49: 1102–11, 1981.

30. **Qiao RL**, **Bhattacharya J**. Segmental barrier properties of the pulmonary microvascular bed. *J Appl Physiol* 71: 2152–2159, 1991. doi: 10.1152/jappl.1991.71.6.2152.

31. **Ying X**, **Minamiya Y**, **Fu C**, **Bhattacharya J**. Ca2+ waves in lung capillary endothelium. *Circ Res* 79: 898–908, 1996. doi: 10.1161/01.res.79.4.898.

32. **Kuebler WM**, **Ying X**, **Singh B**, **Issekutz AC**, **Bhattacharya J**. Pressure is proinflammatory in lung venular capillaries. *J Clin Invest* 104: 495–502, 1999. doi: 10.1172/JCI6872.

33. **Kuebler WM**, **Ying X**, **Bhattacharya J**. Pressure-induced endothelial Ca(2+) oscillations in lung capillaries. *Am J Physiol Lung Cell Mol Physiol* 282: L917-23, 2002. doi: 10.1152/ajplung.00275.2001.

Figure 1: Responses to intranasal *Pseudomonas aeruginosa* in weanling and adult mice

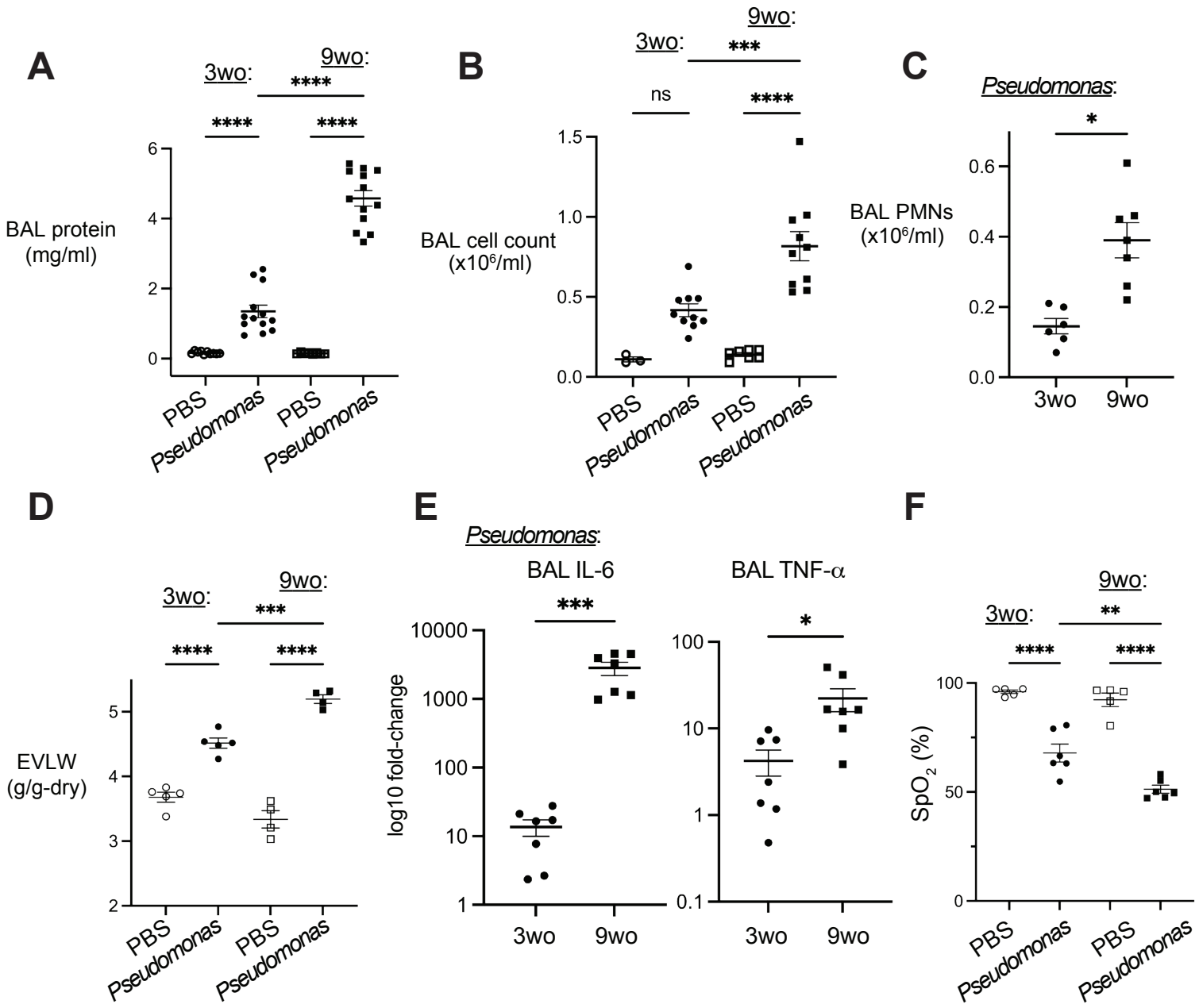

Figure 2: YAP expression responses to *P. aeruginosa*-induced lung injury in weanling and adult mice

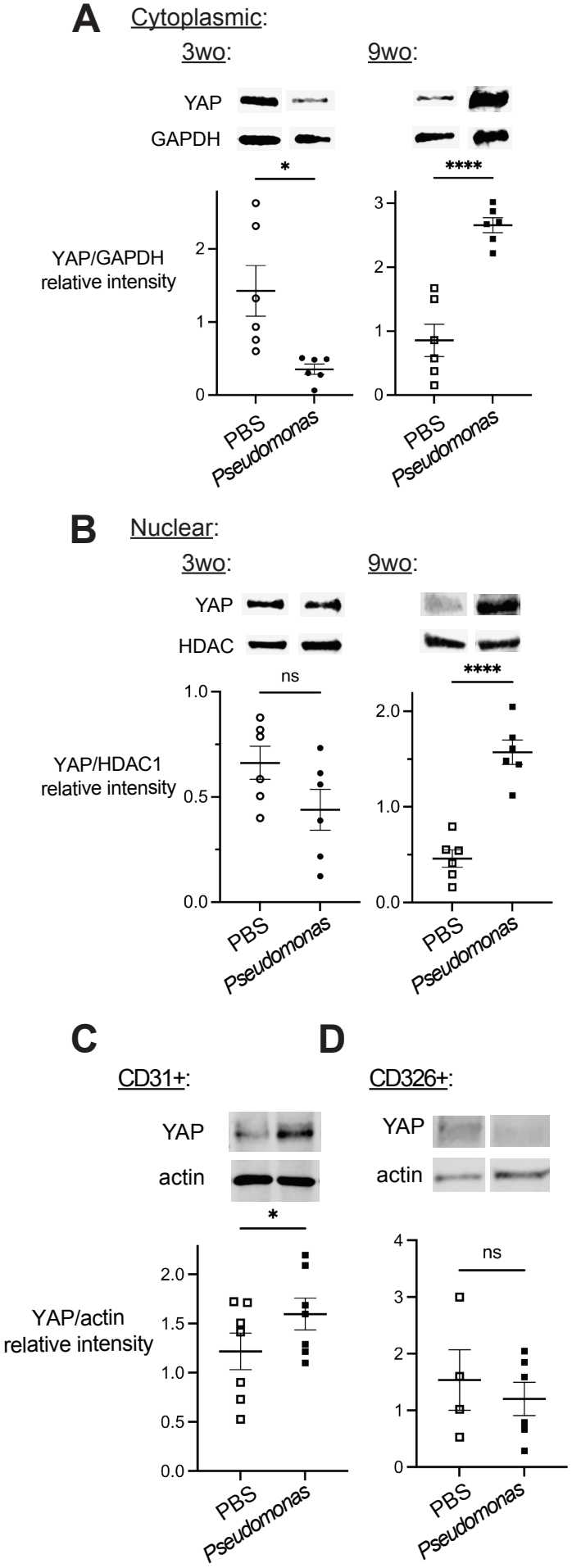

Figure 3: YAP mediates *P. aeruginosa*-induced lung injury in adult mice

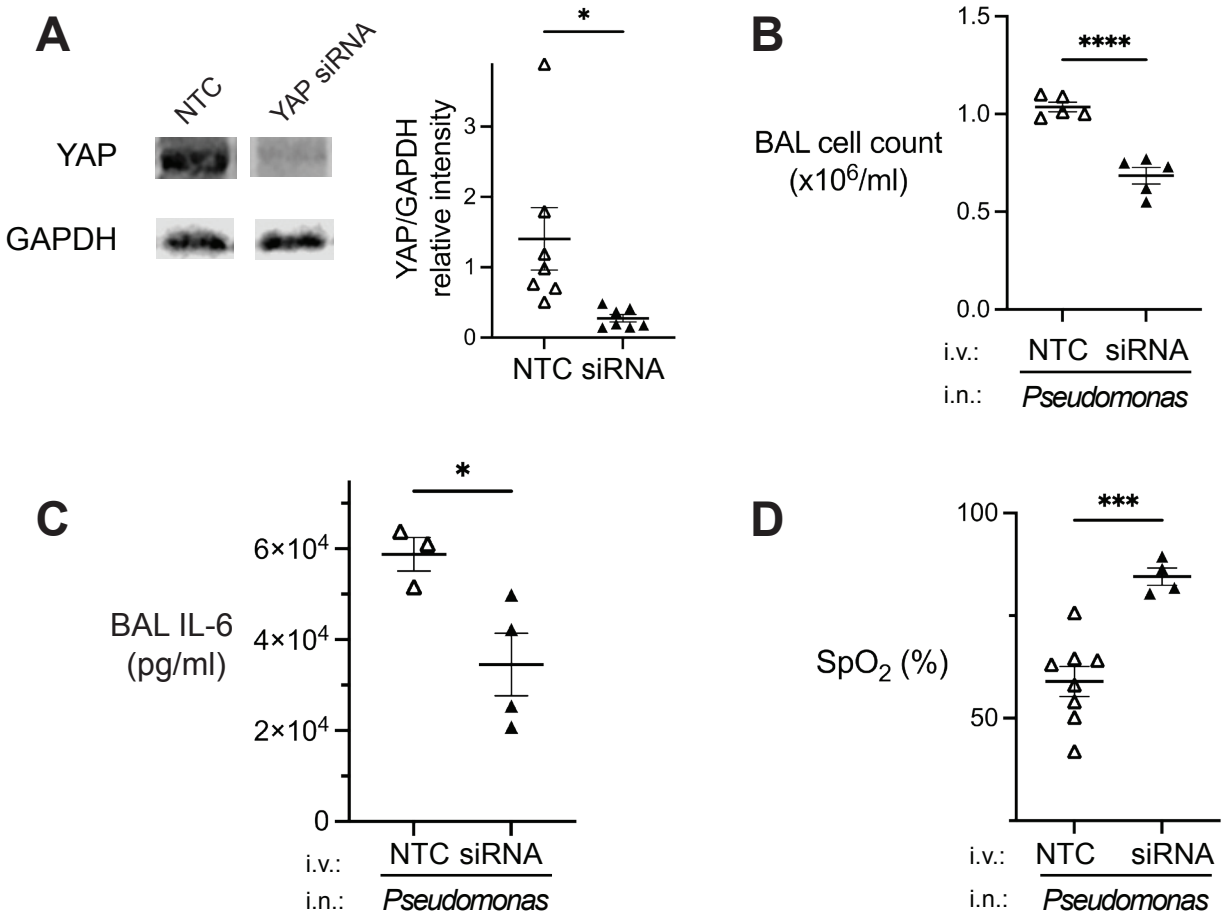
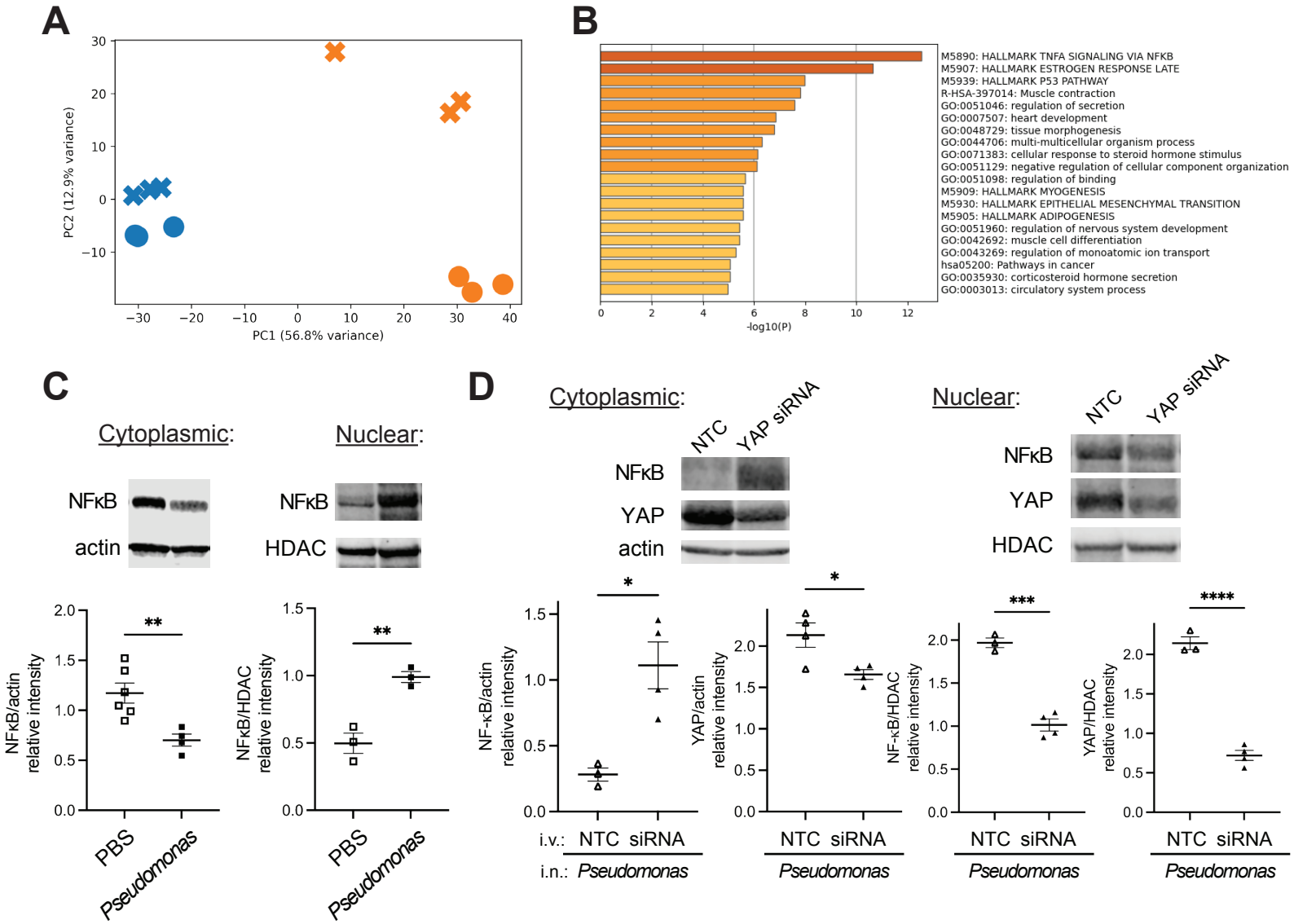
Figure 4: YAP expression drives endothelial NF-κB responses in *P. aeruginosa*-infected adult mice